

# Keratoepithelin Suppresses the Progression of Experimental Human Neuroblastomas

Jürgen Becker,<sup>1</sup> Bernhard Erdlenbruch,<sup>1</sup> Ievgeniia Noskova,<sup>1</sup> Alexander Schramm,<sup>2</sup> Monique Aumailley,<sup>3</sup> Daniel F. Schorderet,<sup>4</sup> and Lothar Schweigerer<sup>1</sup>

<sup>1</sup>Abteilung Pädiatrie I, Zentrum Kinderheilkunde und Jugendmedizin, Klinikum der Georg-August-Universität Göttingen, Göttingen, Germany; <sup>2</sup>Abteilung Hämatologie, Onkologie und Endokrinologie, Universitätsklinikum Essen-Duisburg, Essen, Germany; <sup>3</sup>Institut für Biochemie II und Zentrum für Molekulare Medizin Köln, Universität zu Köln, Köln, Germany; and <sup>4</sup>Institut de Recherche en Ophtalmologie, Department of Ophthalmology, University of Lausanne, Sion, Switzerland

## Abstract

**Neuroblastoma is the most common extracranial childhood tumor. High expression of activin A is associated with a favorable prognosis, but the contributing mechanisms have remained unclear. Our previous demonstration of the activin A-mediated up-regulation of keratoepithelin led to the consideration that keratoepithelin could modulate neuroblastoma growth and/or progression. We report here that enhanced keratoepithelin expression in human neuroblastoma cells suppresses neuroblastoma cell cohesion and adhesion to various extracellular matrix proteins and that it inhibits neuroblastoma cell proliferation and invasion *in vitro* and *in vivo*. Using microarray analysis, we identified several keratoepithelin-regulated genes that may contribute to these biological changes. Together with the observation that keratoepithelin is expressed in human neuroblastomas *in vivo*, our data suggest that keratoepithelin could play a beneficial role in neuroblastoma development and/or progression.** (Cancer Res 2006; 66(10): 5314-21)

## Introduction

Neuroblastoma is the most common extracranial childhood tumor. It is derived from transformed immature sympathetic neuroblasts. Despite aggressive multimodal therapy, mortality has remained in the range of 40%. Although still ill-defined, several molecular derangements may contribute to the poor clinical outcome. These include amplification of the MYCN oncogene, enhanced expression of TrkB, deletions at chromosome 1, and a loss of TrkA or activin A expression (1, 2). We have shown previously that overexpression of MYCN promotes tumor angiogenesis by the concomitant down-regulation of three angiogenesis inhibitors (3). One of these was identified as activin A, a member of the large transforming growth factor- $\beta$  (TGF- $\beta$ ) family of growth and differentiation factors composed of two inhibin  $\beta$ A chains (4). We could show that high expression of activin A correlates with favorable prognosis in human neuroblastoma and markedly up-regulates keratoepithelin (2).

Keratoepithelin (also named  $\beta$ ig-h3, Bigh3, TGF- $\beta$ -induced protein h3, or RGD-CAP) was discovered in adenocarcinoma cell lines as a TGF- $\beta$ -induced secreted 69-kDa protein (5). It is composed of 683 amino acids and accumulates in the extracellular matrix. The

protein includes a NH<sub>2</sub>-terminal signal peptide that is excised during export to the extracellular matrix, four fasciclin-like domains, and a COOH-terminal RGD sequence, which is a putative integrin-binding motif. It has been suggested that keratoepithelin binds to integrins, which are cell surface receptors triggering downstream signaling (6–8), and also to several collagen types (9, 10).

In the past, most studies on keratoepithelin have focused on its mutations and their contributions to the development of corneal dystrophies (11). Recently, however, keratoepithelin was also found to be up-regulated in malignant tissue, including lung (12), esophageal (13, 14), breast (15), and colorectal (16) cancers, suggesting a tumor-supporting role of keratoepithelin. In contrast, transient expression of keratoepithelin in bronchial epithelial tumor cells leads to growth suppression and reduction of integrin  $\alpha_5\beta_1$  expression (17), and keratoepithelin overexpression in Chinese hamster ovary (CHO) cells resulted in reduced tumor proliferation in nude mice (18).

Although these and other data suggest that keratoepithelin may be implicated in tumor development and progression, the role of keratoepithelin in malignancy in general is as yet unclear. In particular, it has remained unclear whether keratoepithelin plays a role in pediatric malignancies. We have therefore examined the molecular and biological consequences of keratoepithelin in neuroblastoma, the most common extracranial childhood malignancy.

## Materials and Methods

If not stated otherwise, all chemicals were purchased from Sigma (Taufkirchen, Germany), Fluka (Buchs, Switzerland), Merck (Schwalbach, Germany), or local suppliers.

**Cell culture.** Kelly and IMR5 neuroblastoma cells were cultured in RPMI 1640 (Cambrex, Verviers, Belgium) containing 1% penicillin/streptomycin and 10% FCS (Biochrom, Berlin, Germany).

Cells transfected with vectors were continuously selected in the above medium containing G418 (100  $\mu$ g/mL; Invitrogen, Carlsbad, CA).

**Cloning of keratoepithelin cDNA.** Keratoepithelin mRNA was isolated from activin A-transfected Kelly cells. Reverse transcription was done using Omniscript reverse transcriptase (Qiagen, Hilden, Germany) according to the provided protocols. The cDNA was then subjected to PCR amplification using the following oligonucleotides, including appropriate restriction sites for cloning into pIRES2-EGFP-vector (BD Biosciences Clontech, Heidelberg, Germany; KE/IRES forward 5'-GTCGAGCTCCATGGCGTCTTC-3' for the *SacI* site and KE/IRES2 reverse 5'-CTGCCGCGGTGCATTCTCTG-3' for the *SacII* site). Restriction enzymes were purchased from MBI Fermentas (St. Leon-Rot, Germany) and T4 ligase from Boehringer (Mannheim, Germany).

Primers were synthesized by MWG Biotech (Ebersberg, Germany).

**Transfection of cells.** Stably transfected cells were established using Superfect reagent (Qiagen). Cells were diluted to 1,000 per 10-cm diameter dish in RPMI 1640 (10% FCS, 1% penicillin/streptomycin, and 600  $\mu$ g/mL G418). When single colonies became visible, they were harvested with trypsin-moistened filter paper confetti and transferred to a 24-well plate for propagation.

**Requests for reprints:** Lothar Schweigerer, Abteilung Pädiatrie I, Zentrum Kinderheilkunde und Jugendmedizin, Klinikum der Georg-August-Universität Göttingen, D-37075 Göttingen, Germany. Phone: 49-551-39-6200; Fax: 49-551-39-6231; E-mail: Lothar.Schweigerer@med.uni-goettingen.de.

©2006 American Association for Cancer Research.  
doi:10.1158/0008-5472.CAN-05-3049

**RNA isolation.** Cells were rinsed once with PBS and harvested with Trizol (Invitrogen) directly from the culture plate. Further RNA isolation was done according to the manufacturer's protocol.

**Real-time reverse transcription-PCR.** Reverse transcription was done with 2  $\mu$ g total RNA using Omniscript reverse transcriptase according to the manufacturer's instructions.

Real-time PCR was done using the qPCR SYBR Green kit (Eurogentec, Seraign, Belgium) on a TaqMan thermocycler (ABI, Foster City, CA) according to the respective manuals.

Primers used were KE forward 5'-TTTATCGTAATAGCCTCTGCATTGA-3' and KE reverse 5'-CATGACAGTCCCCATTGGGG-3', ATF3 forward 5'-CTCTGCGCTGGAATCAGTCA-3' and ATF3 reverse 5'-CCTCGGCTTTGTGATGGA-3', dickkopf 1 (DKK1) sense 5'-AGGAAGCGCCGAAACG-3' and DKK1 reverse 5'-CACACATATTCATTTTGCAGTAATTC-3', Jun dimerization protein 2 (JDP2) sense 5'-AGGGCACCCATCCAAGGA-3' and JDP2 reverse 5'-CCGCGTTTTGGTTGCAA-3', moesin sense 5'-ACTGGGCGGAGACAAATACAA-3' and moesin reverse 5'-AATGCGCTGCTGGTGTG-3', RGS 16 forward 5'-CCTTCAGATACTGTGGGACTCATG-3' and RGS 16 reverse 5'-CCCTCATCATTAGCCCTTATTCA-3', serpin B9 sense 5'-GGCATTGGGAATTGTTGATG-3' and serpin B9 reverse 5'-ACAGGTCTCTCCGCTGACA-3', stanniocalcin 2 (STC2) sense 5'-GGAGCTCCCAGCAGAAAGG-3' and STC2 reverse 5'-TTGACCAACAGTGTGGATCT-3', and TFPI2 sense 5'-CGATGCTTGCTGGAGGATAGA-3' and TFPI2 reverse 5'-ACACTGTCGTCCACACTCACT-3'.

**Microarray experiments.** Expression profiles of keratoepithelin-overexpressing cells (KB 24) and vector control cells (Kelly vec) were done on "G4112A Whole Human Genome Microarrays" (Agilent Technologies, Palo Alto CA).

RNA for this experiment was prepared with the RNeasy kit (Qiagen) as suggested by the manufacturer. Processing of the RNA and labeling was done according to protocols suggested by Agilent.

Each cRNA probe was labeled with Cy3 and Cy5 and hybridized crosswise in a "dye swap" fashion to avoid artifacts due to dye irregularities. Each dye combination was hybridized to arrays in three replicates; six arrays were used for final statistics.

Primary tumor samples of 68 neuroblastoma patients (stage 1:  $n = 20$ ; stage 2:  $n = 16$ ; stage 3:  $n = 7$ ; stage 4:  $n = 15$ ; stage 4s:  $n = 10$ ) were analyzed for keratoepithelin expression by using Affymetrix (Santa Clara, CA) U95A microarrays as described previously (19, 20).

**Western blot analyses.** Cells were scraped in PBS directly from the culture dishes and adjusted to equal numbers. After centrifugation and removal of PBS, the cell pellets were resuspended in deionized water and boiled directly with SDS-PAGE sample buffer containing and DTT. Whole-cell lysates were subjected to SDS-PAGE and transferred to polyvinylidene difluoride membranes (Millipore, Bedford, MA) using a semidry blot device (Biometra, Göttingen, Germany) at 40 mA for 2 hours.

Blots were blocked overnight at 4°C with TBS (pH 7.5) containing bovine serum albumin (5%) and Tween 20 (0.2%). Subsequent incubations with keratoepithelin 2 primary antibody (11) and secondary antibody against rabbit IgG (Dako, Hamburg, Germany; each diluted 1:3,000 in blocking solution) for 1 hour at room temperature were followed by two washing steps with TBS for 10 minutes. Antibody detection was done by chemiluminescence using Enhanced Chemiluminescence reagent (Amersham Biosciences, Little Chalfont, United Kingdom) as recommended by the manufacturer.

**Cell proliferation assays.** Cells ( $10^4$  per well) were seeded into 96-well culture plates in 200  $\mu$ L culture medium. At various times, cells were fixed by adding 50  $\mu$ L of 25% glutaraldehyde. After incubation for 20 minutes, the medium was removed and plates were washed twice with deionized water. The plates were allowed to dry and 100  $\mu$ L crystal violet solution (0.1% in deionized water) was added to each well. After 20 minutes, the dye was removed; the plates were washed thrice with deionized water and dried again. The dye was resolved in 100  $\mu$ L of 10% acetic acid and absorption at 570 nm was determined using a micro plate reader (Molecular Devices, Sunnyvale, CA).

**Cell adhesion assays.** Tissue culture plates (96-well; Costar, Bodenheim, Germany) were coated with triplicate serial dilutions (0-20  $\mu$ g/mL) of laminin 5, collagen I, collagen IV, or fibronectin. After saturation with 1%

bovine serum albumin, equal numbers of KB 24 or Kelly vec cells were seeded on the coated wells. After an incubation period of 30 minutes, cells were fixed, stained with crystal violet, and quantified using a multiplate reader as described previously (21).

For adhesion time kinetics, cells were seeded at equal amounts to 96-well cell culture plates in eight replicates per cell line and time point. At various times, medium and nonadherent cells were aspirated and the remaining adhesive cells were further incubated. Cells were fixed 16 hours after seeding, stained, and quantified as described above.

**Cell invasion and migration assays.** Cells resuspended in serum-free medium ( $5 \times 10^4$  in 500  $\mu$ L) were seeded into BioCoat cell culture inserts (8  $\mu$ m pore size, Becton Dickinson, San Diego, CA) with or without Matrigel coating on the upper side. The inserts were placed into a 24-well cell culture plate with RPMI 1640 containing FCS (20%). After 72 hours, cells that had crossed the membrane were stained with hematoxylin. The cell number was counted microscopically at  $\times 200$  magnification in four fields (north, east, south, and west) of each membrane.

**Spheroid assays.** Spheroids were established as described (22). In brief, cells were harvested from culture plates and quantified. Cells were diluted to 1:000 per 100  $\mu$ L medium containing 10% Methocel (basal medium containing 2.4% methylcellulose). Cell suspension (100  $\mu$ L) was seeded to each well of 96-well U-shaped cell culture plates for suspension cell cultures. Spheroids were allowed to form and grow for 10 days at 37°C and 5% CO<sub>2</sub>.

**Spheroid outgrow in Matrigel.** Multiwell plates were coated with 50  $\mu$ L ice-cold Matrigel (BD Biosciences, San Diego, CA) and incubated for 30 minutes at 37°C. Ten-day-old spheroids were set on the hardened Matrigel by using cutoff pipette tips. The spheroids were then overlaid with 50  $\mu$ L Matrigel and placed into a cell incubator at 37°C under 5% CO<sub>2</sub>. After the top layer was hardened, 100  $\mu$ L cell culture medium (see above) was gently applied to each well. Every second day, the medium was aspirated and replaced by fresh medium. Growth was documented by digital microscopy photography using Leica equipment (Leica, Bensheim, Germany).

**Chick chorioallantoic membrane assays.** These experiments were done essentially as described previously (23).

**Animal experiments.** Cells ( $10^7$  in Matrigel) were injected s.c. into nude mice. The animal's weight and tumor volumes were determined every second day. Tumor volumes were quantified using venire calipers. Volumes were estimated using the formula:  $V_{\text{tumor}} = \text{height} \times \text{length} \times \text{width} \times 0.7$ . Animals were sacrificed when the tumor volume exceeded 2.5 cm<sup>3</sup> or when day 42 of the experiments was reached. All animal experiments were done according to guidelines of local and national authorities.

## Results

We have shown recently that the prognostically unfavorable MYCN oncogene can down-regulate activin A in human neuroblastoma cells, that activin A inhibits growth and angiogenesis of experimental human neuroblastomas, and that activin A up-regulates keratoepithelin (2). These data suggested that MYCN loss could permit up-regulation of activin A and that the subsequent up-regulation of keratoepithelin could contribute to the beneficial effects of activin A in human neuroblastoma. To support this hypothesis, we established gene expression profiles of human neuroblastoma samples ( $n = 68$ ) using Affymetrix arrays. Although we found no significant correlation between keratoepithelin mRNA levels and outcome or clinical stages (data not shown), we were able to show a significant correlation ( $P < 0.05$ ) of MYCN amplification with decreased keratoepithelin mRNA expression. To substantiate our hypothesis, we attempted to develop an experimental system using neuroblastoma cells with or without keratoepithelin expression.

**Keratoepithelin overexpression in human neuroblastoma cell lines.** For stable overexpression of keratoepithelin, we selected the human neuroblastoma cell line Kelly (2). Among the successful transfectants, we chose two cell clones with moderate (KB 16) or

high (KB 24) keratopithelin expression levels. Using real-time reverse transcription-PCR (RT-PCR), we found keratopithelin transcript levels in the KB 16 or KB 24 clones to be ~20- to 150-fold above those in untransfected wild-type (Kelly wt) or Kelly vec control cells (Fig. 1A). That keratopithelin expression resulted in keratopithelin protein synthesis was confirmed by Western blot analysis, showing 70-kDa keratopithelin immunoreactive protein doublets in lysates of KB 16 or KB 24 but not Kelly wt or Kelly vec cells, respectively (Fig. 1B). The duplex bands probably reflect the presence of both the immature 78-kDa and the processed 69-kDa keratopithelin lacking the NH<sub>2</sub>-terminal signal peptide. To examine whether keratopithelin is also released from the cells, we examined concentrated cell supernatants for the presence of keratopithelin. As expected, keratopithelin immunoreactivity was present in supernatants of the keratopithelin-transfected but not the control cells (Fig. 1C). There was only one major keratopithelin immunoreactive band detectable in conditioned medium, supporting the hypothesis that the duplex band in Fig. 1B is due to processing into the mature protein.

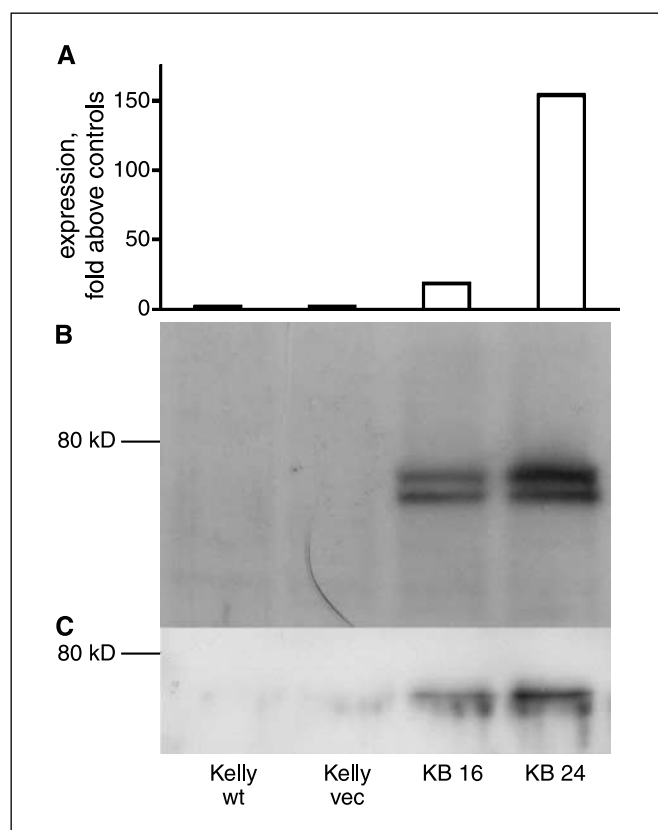


**Figure 1.** Analysis of keratopithelin expression in transfected human neuroblastoma cells. Kelly neuroblastoma cells (Kelly wt) were transfected with either an empty vector (Kelly vec) or the vector containing keratopithelin cDNA (KB 16 and KB 24). *A*, cells were harvested and mRNA and cDNA were prepared as described in Materials and Methods. Keratopithelin expression levels were determined by quantitative real-time RT-PCR using SYBR Green. Expression levels are given as relative expression when compared with the control cells (Kelly wt; i.e., 1). *B*, cell lysates were separated by SDS-PAGE and subjected to Western blot analysis using specific antibodies against keratopithelin as described in Materials and Methods. *C*, conditioned serum-free medium was harvested after 48 hours and concentrated 10-fold with a 10-kDa cutoff membrane centrifugation unit and subjected to Western blotting and immunodetection as described in Materials and Methods. *B* and *C*, representative of at least three separate experiments.

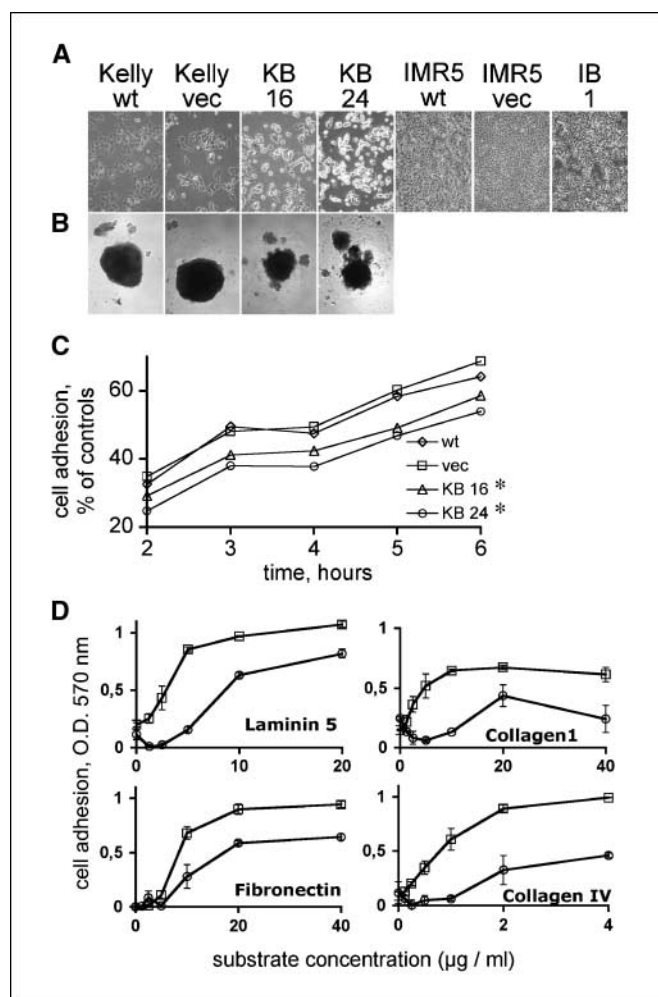


**Figure 2.** Effect of keratopithelin on adhesion and cohesion. Microscopic view of the (*A*) morphology (magnification,  $\times 200$ ) or (*B*) spheroid-forming capacities (magnification,  $\times 100$ ) of wild-type (Kelly wt) or vector (Kelly vec) controls of the keratopithelin-expressing transfectants (KB16 or KB24, respectively). Cells were cultured as described in Materials and Methods. Spheroids were monitored after 10 days. *C*, effect of time on cell attachment to culture dishes. Cells ( $5 \times 10^4$ ) of the indicated cell lines were seeded on 96-well plates. At the indicated times, cells were fixed and stained with crystal violet and cell numbers were determined photometrically at 570 nm in a plate reader. Adherent cells are indicated as percentage of the respective control. \*,  $P < 0.05$  for transfected versus control cells. Representative of three experiments. *D*, effect of various substrate concentrations on cell attachment. Kelly vec or KB 24 cells were seeded on 96-well plates, which had been precoated with different substrates at the indicated concentrations. Cell numbers were determined in triplicate as described in Materials and Methods. Points, mean; bars, SD.

**Keratopithelin modulates cell morphology.** The keratopithelin-expressing neuroblastoma cell clones KB 16 and KB 24 but not the control cells (Kelly wt and Kelly vec) appeared opalescent and round (Fig. 2A), suggesting that keratopithelin modulates cell adhesion and/or cohesion.

**Keratopithelin suppresses cell cohesion.** The latter hypothesis was tested using a spheroid assay. Cells were seeded into U-shaped uncoated cell culture dishes, thus preventing cellular adhesion and promoting cellular spheroid generation exhibiting intact cell-cell adhesion properties. Whereas Kelly wt and Kelly vec cells were able to form compact, round-shaped spheroids, KB 16 and KB 24 cells were unable to do so and rather formed small, irregular, and friable aggregates (Fig. 2B), suggesting that keratopithelin attenuates cohesion of human neuroblastoma cells.

**Keratoepithelin impairs cell adhesion.** To determine whether keratoepithelin also modulates neuroblastoma cell adhesion, we quantified the ability of cells to adhere to culture dishes as a function of time. As shown in Fig. 2C, the keratoepithelin-expressing cell clones KB 16 and KB 24 had reduced adhesive potentials ( $P < 0.05$ ) when compared with the control cells. To identify the molecular mechanisms by which keratoepithelin alters neuroblastoma cell adhesion, we examined the integrin-mediated ability of the neuroblastoma cell clone KB 24 to adhere to various extracellular matrix proteins, including laminin 5, fibronectin, collagen I, and collagen IV. When compared with the controls (Kelly vec), KB 24 cells had a reduced ability to adhere to all proteins tested, suggesting a general rather than a specific adhesive defect in keratoepithelin-expressing cells (Fig. 2D).

**Keratoepithelin inhibits invasion *in vitro*.** The results presented above suggested that keratoepithelin could also modulate invasion of human neuroblastoma cells. To test this hypothesis, we examined the abilities of the KB 16 or KB 24 neuroblastoma clones to invade extracellular matrix-containing gels (Matrigel). When compared with the controls (Kelly wt/Kelly vec), the keratoepithelin-expressing cell clones were barely able to cross the gel and their invasive potentials were in the range of only 20% to 50% of that of the controls (Fig. 3A). Remarkably, there was no difference in the migratory potency of keratoepithelin-expressing and control cells when tested on uncoated membranes (data not shown). We therefore assumed that keratoepithelin might suppress invasion rather than migration.

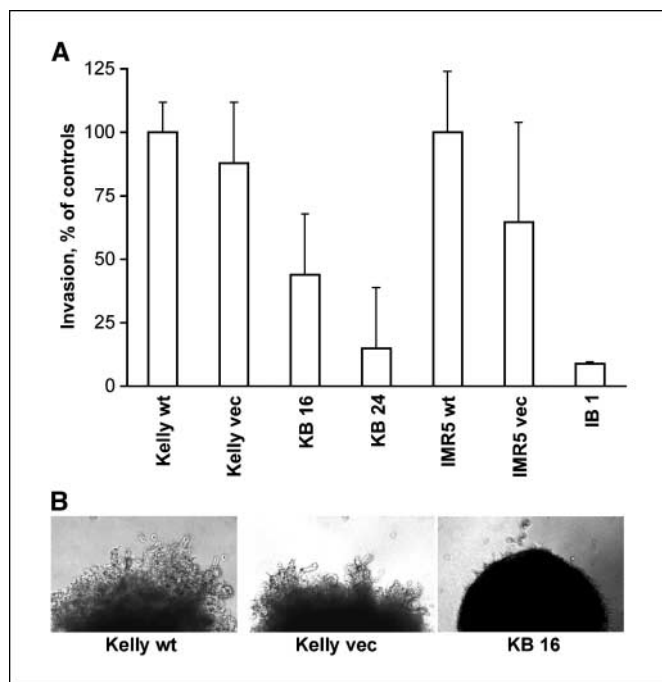


**Figure 3.** Effect of keratoepithelin expression on invasion. *A*, cell invasion through Matrigel-coated membranes. Cells ( $10^5$ ) in serum-free medium were seeded in BioCoat Matrigel invasion chamber inserts and examined for their invasive capacities as described in Materials and Methods. Representative of one of three experiments. *Columns*, mean; *bars*, SD. *B*, invasion of cells from spheroids into surrounding Matrigel. Ten-day-old spheroids derived from Kelly wt, Kelly vec, or KB 16 cells were placed in Matrigel as described in Materials and Methods. Pictures were taken at day 12 (magnification,  $\times 100$ ). Spheroids of the KB 24 cells were not tested because due to their low cohesion properties they could not be transferred into the Matrigel without breaking.

To verify this hypothesis, we used a modified spheroid assay in which the tumor cell spheroids are implanted into Matrigel. Again, cells from spheroids of Kelly wt and Kelly vec cells invaded the surrounding matrix and became visible at the edge of the spheroid. In contrast, KB 16 cells barely invaded the gels (Fig. 2B). Spheroids of KB 24 cells (with high keratoepithelin expression) were too friable for transfer into Matrigel and could not be tested.

**Keratoepithelin inhibits cell proliferation.** For further characterization of the keratoepithelin-expressing cell lines, we compared the proliferation rates of KB 16 and KB 24 with those of the control (Kelly wt and Kelly vec) cells *in vitro* (Fig. 4A). Whereas proliferation rates of the controls were similar, those of the KB 16 and KB 24 clones were considerably lower and ranged between only 60% and 75% of the controls (Fig. 4A). Similar results were obtained when cell numbers were determined using a Coulter particle counter (data not shown).

**Keratoepithelin inhibits tumor growth *in vivo*.** The results obtained using *in vitro* methods suggested that keratoepithelin could suppress tumor growth and progression *in vivo*. To test this hypothesis, we used two different methods [i.e., the chorioallantoic membrane (CAM) assay in the chick embryo and the mouse tumor assay]. The CAM represents a natural epithelial barrier that can only be overcome by highly invasive tumor cells. The successful tumor cells have then the ability to proliferate and expand beyond a size of a few millimeters. However, expansion depends critically on the angiogenic potential of the cells. When KB 16, KB 24, and control (Kelly wt and Kelly vec) cells were seeded onto the CAM, visible tumors developed in 60% of the embryos, which had received control cells, but in only 20% ( $P < 0.05$ ) of the embryos, which had received KB 16 or KB 24 cells, respectively (Fig. 4C). In addition, KB 16- or KB 24-derived tumors were considerably smaller than those derived from the control cells (data not shown). Thus, keratoepithelin suppresses invasion and progression of experimental human neuroblastomas.

To exclude artifacts related to the methodology, we sought to confirm these data using a second animal model. After injecting the neuroblastoma cells s.c. into nude mice, we compared the tumor-forming abilities of KB 16 and KB 24 cells with those of control cells (Kelly wt and Kelly vec). Again, Kelly wt and Kelly vec cells rapidly formed visible tumors, whereas the KB 16 or KB 24 clones were unable to do so ( $P < 0.05$ ; Fig. 4D). On explantation, we observed that tumors derived from control cells were well-vascularized and occasionally included necrotic areas, whereas tumors derived from the KB 16 or KB 24 clones were small and sometimes had not grown beyond the *in situ* stage (Fig. 4D, insets; data not shown).

To verify the potential general nature of our results, we established a second keratoepithelin-expressing cell line based on the human neuroblastoma cell line IMR5. We chose a clonal cell line (IB 1) with high keratoepithelin expression as confirmed by Western blot analysis (data not shown). Like the keratoepithelin-expressing KB 16 and KB 24, the IB 1 cells appeared more opalescent than the IMR5 parental cells (IMR5 wt) or vector controls (IMR5 vec; Fig. 2B). IB 1 cells were  $\sim 80\%$  less invasive than IMR5 wt and IMR5 vector control cells (Fig. 3A). Proliferation of IB 1 cells was also reduced by  $\sim 75\%$  compared with the controls (IMR5 wt and vec; Fig. 4B). Overall, experiments with keratoepithelin-expressing IMR5 cells gave results very similar to those obtained by experiments with KB 16 and KB 24 cells, indicating that our results are of general relevance rather than being a function of a specific cell line.

In summary, we have shown here that keratopithelin suppresses neuroblastoma cell proliferation and progression in several experimental settings. Because identification of the underlying molecular mechanisms could be of future relevance in terms of neuroblastoma diagnosis and therapy, we compared gene expression profiles of the keratopithelin-expressing KB 16 and KB 24

cells with those of the control cells using Whole Human Genome Microarrays (G4112A). Statistical analysis of the data obtained revealed 102 differentially (by a factor >2) regulated genes (data not shown). Of these, 65 genes were apparently up-regulated and 37 down-regulated in the keratopithelin-expressing cells (data not shown). Of the 102 potential targets, 28 were unknown transcripts with no available annotations and were therefore not further considered. The remainders were sequences whose corresponding genes are implicated in various activities, including signaling, adhesion, migration, invasion, or tumor progression. From these genes, the most interesting with regard to expression levels and/or gene function were selected for validation by real-time RT-PCR. The results revealed that some of the selected genes were obviously not consistently regulated between Kelly wt and Kelly vec or KB 16 and KB 24, respectively, and therefore rated as "false positives." However, eight transcripts could be validated (Table 1) and their qualitative regulation matched that found by microarray analyses. The *JDP2*, *TFPI2*, *DKK1*, *STC2*, *ATF3*, and *RGS 16* genes were up-regulated in KB 16 and KB 24 cells, whereas the *moesin* and *serpin B9* genes were down-regulated. Some of these genes (*JDP2*, *TFPI2*, and *serpin B9*; cf. Table 1) were regulated in a dose-dependent manner.

## Discussion

Thus far, knowledge about the potential role of keratopithelin in solid malignancies is fragmentary and controversial. Recently, we showed for the first time that activin A up-regulates keratopithelin in human neuroblastoma cells (2). Here, we sought to elucidate the potential functional consequences of keratopithelin expression in human neuroblastoma. For our experiments, we chose the highly malignant and well-characterized human neuroblastoma cell line Kelly (24). By transfection with a keratopithelin-containing vector, we obtained two cell clones with stable moderate to high keratopithelin expression, named KB 16 and KB 24 (Fig. 1). The derived cell lines KB 16 and KB 24 exhibited a reduced potential to adhere to standard cell culture dishes (Fig. 2A and C). One might argue that adhesion differences between control cells and keratopithelin-expressing cells ( $P < 0.05$ ) occur before 2 hours after plating the cells (cf. Fig. 2C). However, based on our observation during maintenance of the cells, we think that the differences in cell adhesion in Fig. 2C do not arise because there are fewer cells attached to the plate but rather because adhesion strength of the keratopithelin transfected cells is significantly lower than in control cells, although they share a similar time course. KB 24 cells were also tested for their ability to adhere to specific substrates, including fibronectin, laminin 5, collagen I, and collagen IV (Fig. 2D).

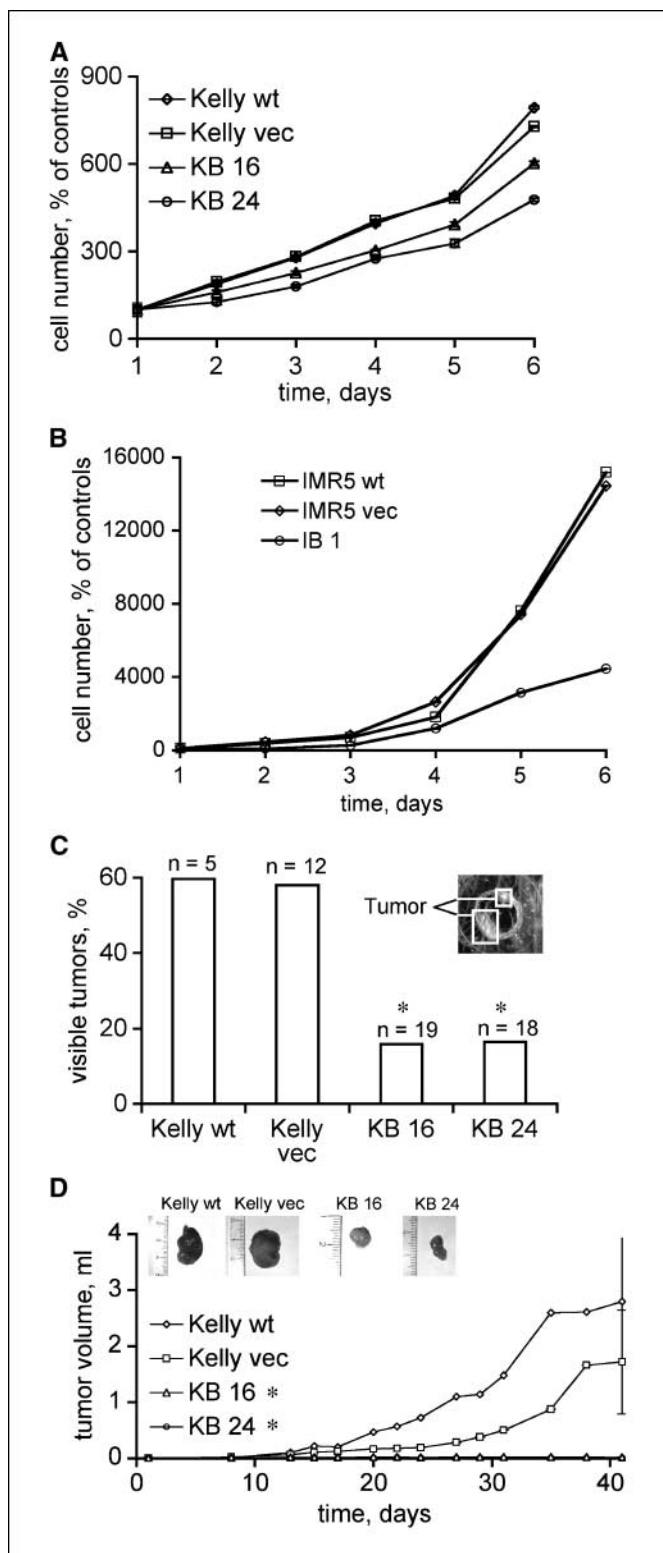


**Figure 4.** Effect of keratopithelin expression on proliferation. *A* and *B*, *in vitro*,  $5 \times 10^3$  cells each were seeded in eight replicates into 96-well plates. At the indicated times, cells were fixed and stained with crystal violet and dye accumulation was quantified at 570 nm. Cell proliferation was calculated as percent value of the absorbance at day 1 for each cell line. Representative of three experiments. Points, mean; bars, SD (hidden by the symbols). *C*, *in vivo*, cells were seeded on the CAM of 10-day-old chick embryos. After 8 days, tumor formation was macroscopically evaluated and any visible tumor (magnification,  $\times 40$ ) was counted. Tumor formation is given as percent of the number of evaluated eggs ( $n$ ). \*,  $P < 0.05$  for KB 16/KB 24 versus Kelly wt/vec. Inset, representative tumor derived from Kelly wt cells. *D*, *in vivo*,  $10^7$  cells of either cell line were injected s.c. into immunodeficient mice as described in Materials and Methods. Points, mean tumor volumes; bars, SE for the average final tumor volume (for KB 16 and KB 24 hidden by symbols). \*,  $P < 0.05$  for Kelly wt/vec versus KB16/24. Insets, representative tumors derived from the indicated cell lines.

**Table 1.** Quantification of the expression of keratoepithelin-regulated gene transcripts by real-time RT-PCR

	Kelly wt	Kelly vec	KB 16	KB 24
<b>Up-regulated</b>				
<i>ATF3</i>	0.931 ± 0.193	1.000 ± 0.000	2.024 ± 0.418	2.457 ± 0.800
<i>DKK1</i>	0.596 ± 0.046	1.000 ± 0.000	3.275 ± 0.359	2.035 ± 0.223
<i>JDP2</i>	0.574 ± 0.010	1.000 ± 0.000	1.444 ± 0.025	1.815 ± 0.019
<i>RGS 16</i>	0.746 ± 0.080	1.000 ± 0.000	1.702 ± 0.513	1.643 ± 0.397
<i>STC2</i>	0.887 ± 0.197	1.000 ± 0.000	2.362 ± 0.885	2.698 ± 0.559
<i>TFPI2</i>	0.404 ± 0.052	1.000 ± 0.000	1.529 ± 0.103	2.891 ± 0.541
<b>Down-regulated</b>				
<i>Moesin</i>	0.321 ± 0.018	1.000 ± 0.000	0.161 ± 0.008	0.184 ± 0.017
<i>Serp1n B9</i>	0.432 ± 0.091	1.000 ± 0.000	0.248 ± 0.041	0.100 ± 0.017

NOTE: Expression levels of eight selected transcripts are given for each cell line as a multiple of expression in control cells (Kelly vec). Each sample was tested in triplicate and every test was repeated thrice with cDNA from independent biological replicates. Average relative expression levels were calculated as the mean ± SD of three independent experiments.

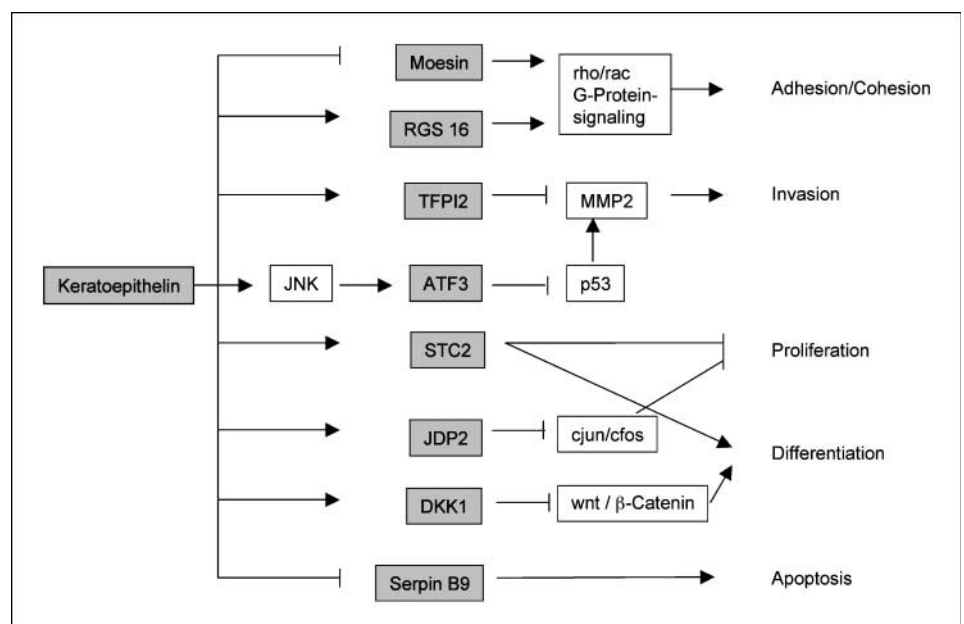
Interestingly, keratoepithelin has been reported previously to bind to collagen (9, 10), and we found a general inability of the keratoepithelin-expressing cells for adherence. As shown here by spheroid-forming assays (Fig. 2B), keratoepithelin-expressing cells are also defective in cell-cell interaction. Keratoepithelin was proposed to function as a cell adhesion molecule based on the observation that keratoepithelin coating promoted cells adhesion presumably by interaction with cellular integrins (6, 25). It seems possible that binding of integrins to precoated keratoepithelin enhances adhesion, whereas expression of keratoepithelin within cells blocks the cells' own integrins, thereby preventing adhesion to substrates and cell-cell contacts. However, judging from our microarray data, other molecular mechanisms may also contribute to the adhesion defect of keratoepithelin-expressing cells (Fig. 5).

The ability to invade adjacent normal tissue is a key prerequisite for malignant tumor progression. We therefore tested the invasive potential of the keratoepithelin-expressing cell lines KB 16 and KB 24 (Fig. 3). Using two different methods (i.e., Matrigel-coated

chambers and spheroids embedded in Matrigel), we showed that keratoepithelin-expressing neuroblastoma cells are considerably less invasive than control cells with no keratoepithelin expression and these effects are apparently dose-dependent (cf. Fig. 1).

Nam et al. have reported previously that blocking  $\alpha_v\beta_3$  integrin by antibodies or a synthetic peptide from the keratoepithelin sequence inhibits migration of endothelial cells (8). We could not find a difference in migration among KB 16, KB 24, and the control cell lines (data not shown), suggesting that this antimigratory effect of keratoepithelin may be restricted to endothelial cells. In further experiments, we examined the proliferative properties of KB 16 and KB 24 cells. *In vitro*, both cell lines are clearly growth inhibited compared with Kelly wt and Kelly vec cells (Fig. 4A) and the rate of inhibition correlates with the amounts of keratoepithelin expressed (see Fig. 1). This result may conflict with recently published results, where renal epithelial cells showed enhanced proliferation when they were seeded on keratoepithelin-coated dishes (26). In early studies, Skonier et al. made the observation that keratoepithelin is

**Figure 5.** Proposed model of keratoepithelin-induced alterations in neuroblastoma cells. Gray boxes, keratoepithelin-regulated molecules; white boxes, proposed intermediate signals; arrowheads, activating signals; blunt lines, inhibitory signals. See discussion for detailed explanation.



mainly expressed in slow-growing tumor cells. Thus, their data match our results (5).

We have also transfected a second cell line, IMR5, to establish stably keratopithelin-expressing cells. These cells, called IB 1, appeared more opalescent than control cells under standard cell culture conditions (Fig. 2A). They are less invasive (Fig. 3A) and proliferate slower compared with control cells (IMR5 wt and IMR5 vec). Taken together, keratopithelin expression in IMR5 cells causes a phenotype very similar to that in Kelly cells and both cell lines exhibit very similar behavior *in vitro*. We therefore conclude that our findings are representative and relevant.

To test the relevance of keratopithelin expression *in vivo*, we first chose the chick CAM model (Fig. 4C). Kelly wt and Kelly vec cells seeded on the CAM of chicken embryos were able to form visible tumors in 60% of the tested embryos. In KB 16 and KB 24 cells, tumor formation was reduced to 20% ( $P < 0.05$ ) and the few tumors were barely visible. A similar observation was made when we injected the cells s.c. into nude mice (Fig. 4D). There was barely tumor formation of KB 16 and KB 24 cells ( $P < 0.05$ ), whereas Kelly wt and Kelly vec cells rapidly formed huge tumors. Therefore, our results suggest an important effect of keratopithelin on tumor progression *in vivo*. Similar results were published for keratopithelin-expressing CHO cells in nude mice (18). However, to our knowledge, this is the first time that keratopithelin-expressing tumor cells have been tested using *in vivo* models.

Keratopithelin is believed to exert its effects on migration, proliferation, and adhesion via interaction with integrins (6–8). Thus far, however, nothing is known about the potential downstream mediators of the assumed keratopithelin-integrin signaling pathway.

Comparison of expression profiles from Kelly vec and KB 24 cells and subsequent validation of selected genes suggested some of the molecular mechanisms, which might be triggered in keratopithelin-expressing neuroblastoma cells (Fig. 5). For example, moesin, a member of the ezrin-radixin-moesin complex linking the cytoskeleton to the membrane, participating in Rho/Rac-mediated signal transduction, and contributing to cell shaping, cell-matrix, and cell-cell adhesion as well as spreading and motility of malignant cells (27, 28), is down-regulated in KB 16 and KB 24 cells (Table 1). RGS 16, which was found to be up-regulated in both keratopithelin-expressing cell lines, may also influence cell-cell and cell-matrix interactions, as it limits signals from G-protein-coupled receptors by activation of GTPases (29). Because G-protein signaling is also implicated in the moesin action, both moesin and RGS 16 may (at least in part) contribute to the reduced adhesion/cohesion of keratopithelin-expressing cells. We have also shown that keratopithelin suppresses invasion *in vitro* and *in vivo* (Figs. 3 and 4B and C) and up-regulates TFPI2 and ATF3 (Table 1). Because TFPI2 inhibits invasion and migration [presumably by inhibiting the activities of plasmin and matrix metalloproteinases (MMP); refs. 30–32] and ATF3 inhibits MMP-2 expression (33), the keratopithelin-mediated up-regulation of both molecules could contribute to the suppression invasion and tumor formation in KB 24 and KB 16 cells (Fig. 5).

Keratopithelin also up-regulates molecules involved in cell differentiation and proliferation. These include DKK1, STC2, and JDP2. DKK1 is a potent inhibitor of the Wnt/ $\beta$ -catenin pathway and deregulation of Wnt signaling is thought to contribute to the development of numerous human cancers by shifting the tumor cells back to a “stem cell-like” proliferative state (34). This opinion is supported by the finding that inhibition of Wnt signaling by DKK1 leads to an increased expression of epithelial differentiation

markers (35) and a recent publication by Oh et al., suggesting a role for keratopithelin in keratinocyte differentiation (36).

STC is a glycoprotein hormone involved in fish mineral homeostasis, but its function in vertebrates is still unclear. Human STC2, which is closely related to STC, was found to correlate with favorable prognosis in estrogen receptor-positive breast cancer (37) and expression in transgenic mice induces inhibition of embryonic growth (38). Although these data suggest a favorable role for STC2 in tumor development, Wong et al. reported STC2 to be down-regulated in Neuro2A mouse neuroblastoma cells during dibutyl cyclic AMP-triggered differentiation (39). This suggests that STC2 rather contributes to an undifferentiated malignant phenotype and raises the need for further investigations on STC2 function in neuroblastoma.

JDP2 is a regulator of the c-Jun/c-Fos signaling pathway. It is able to dimerize with c-Jun and thus inhibits formation of the AP1 transcription activating complex (40). It has been shown that JDP2 prevents cell transformation by Ras and inhibits tumor cell growth in nude mice (41). Additionally, JDP2 expression inhibits cell cycle progression in rhabdomyosarcoma and induces muscle cell differentiation (42). These data indicate that JDP2 may also contribute to the phenotype of keratopithelin-expressing cells by regulating the expression of other molecules. The last example for regulated genes we found is serpin B9, a member of the serine protease inhibitor family that inhibits granzyme B-mediated apoptosis (43, 44). As treatment of CHO and H1299 cells with RGD peptides from keratopithelin was shown to induce apoptosis (45), this might be in part due to serpin B9 down-regulation. By fluorescence-activated cell sorting analysis, we could not find significant differences in apoptosis between keratopithelin-expressing and control cells (data not shown). It seems possible that despite there is no increase in apoptosis the cells might have an increased susceptibility for apoptotic stimuli.

In summary, our data suggest that keratopithelin is an important mediator of the activin A-induced beneficial changes in neuroblastomas by shifting the cells toward a benign phenotype characterized by decreased adhesion, invasion, and proliferation *in vitro*. We have also shown for the first time that stable expression of keratopithelin in human neuroblastoma cells causes a dramatic inhibition of tumor formation and progression *in vivo*. This shift of the phenotype from malignant to benign is accompanied by changes in the expression levels of several genes known to be relevant for adhesion, invasion, proliferation, and tumor progression. Our data were raised with two independent cell clones expressing different quantities of keratopithelin. That keratopithelin expression correlated in a quantitative manner with the functional consequences supports the notion that they are not artifactual but, in fact, keratopithelin specific.

In array experiments and immunohistochemical analyses (data not shown) with samples from 68 patients, we found keratopithelin being expressed in some but not all neuroblastomas. We found no significant correlation with the stage of disease or patient outcome (data not shown) but rather an inverse correlation between expression levels of the MYCN oncogene and keratopithelin. Future investigations are necessary to elucidate the clinical effect of keratopithelin in neuroblastoma as well as the underlying signaling pathways and potential effector molecules.

## Acknowledgments

Received 8/31/2005; revised 1/23/2006; accepted 3/13/2006.

**Grant support:** Wilhelm-Sander-Stiftung, McDonald's Kinderhilfe.

The costs of publication of this article were defrayed in part by the payment of page charges. This article must therefore be hereby marked *advertisement* in accordance with 18 U.S.C. Section 1734 solely to indicate this fact.

We thank Joerg Wilting and Maria Papoutsi for providing the chicken model, Thomas Korff for providing the spheroid model, Peter Zezula for statistical surveillance, and Hoa Nguyen and Monika Pesch for excellent technical assistance.

## References

1. Brodeur GM. Neuroblastoma: biological insights into a clinical enigma. *Nat Rev Cancer* 2003;3:203-16.
2. Schramm A, von Schuetz V, Christiansen H, et al. High activin A-expression in human neuroblastoma: suppression of malignant potential and correlation with favourable clinical outcome. *Oncogene* 2005;24:680-7.
3. Fotis T, Breit S, Lutz W, et al. Down-regulation of endothelial cell growth inhibitors by enhanced MYCN oncogene expression in human neuroblastoma cells. *Eur J Biochem* 1999;263:757-64.
4. Breit S, Ashman K, Wilting J, et al. The N-myc oncogene in human neuroblastoma cells: down-regulation of an angiogenesis inhibitor identified as activin A. *Cancer Res* 2000;60:4596-601.
5. Skonier J, Neubauer M, Madisen L, Bennett K, Plowman GD, Purchio AF. cDNA cloning and sequence analysis of  $\beta$ ig-h3, a novel gene induced in a human adenocarcinoma cell line after treatment with TGF- $\beta$ . *DNA Cell Biol* 1992;11:511-22.
6. Kim JE, Kim SJ, Lee BH, Park RW, Kim KS, Kim IS. Identification of motifs for cell adhesion within the repeated domains of transforming growth factor- $\beta$ -induced gene, betaig-h3. *J Biol Chem* 2000;275:30907-15.
7. Kim JE, Jeong HW, Nam JO, et al. Identification of motifs in the fasciclin domains of the transforming growth factor- $\beta$ -induced matrix protein betaig-h3 that interact with the  $\alpha_v\beta_3$  integrin. *J Biol Chem* 2002;277:46159-65.
8. Nam JO, Kim JE, Jeong HW, et al. Identification of the  $\alpha_v\beta_3$  integrin-interacting motif of betaig-h3 and its anti-angiogenic effect. *J Biol Chem* 2003;278:25902-9.
9. Hashimoto K, Noshiro M, Ohno S, et al. Characterization of a cartilage-derived 66-kDa protein (RGD-CAP/ $\beta$ ig-h3) that binds to collagen. *Biochim Biophys Acta* 1997;1355:303-14.
10. Hanssen E, Reinboth B, Gibson MA. Covalent and non-covalent interactions of betaig-h3 with collagen VI.  $\beta$ ig-h3 is covalently attached to the amino-terminal region of collagen VI in tissue microfibrils. *J Biol Chem* 2003;278:24334-41.
11. Korvatska E, Munier FL, Chaubert P, et al. On the role of kerato-epithelin in the pathogenesis of 5q31-linked corneal dystrophies. *Invest Ophthalmol Vis Sci* 1999;40:2213-9.
12. Sasaki H, Kobayashi Y, Nakashima Y, et al.  $\beta$ IGH3, a transforming growth factor- $\beta$  inducible gene, is overexpressed in lung cancer. *Jpn J Clin Oncol* 2002;32:85-9.
13. Hourihan RN, O'Sullivan GC, Morgan JG. Transcriptional gene expression profiles of oesophageal adenocarcinoma and normal oesophageal tissues. *Anticancer Res* 2003;23:161-5.
14. Hu YC, Lam KY, Law S, Wong J, Srivastava G. Profiling of differentially expressed cancer-related genes in esophageal squamous cell carcinoma (ESCC) using human cancer cDNA arrays: overexpression of oncogene MET correlates with tumor differentiation in ESCC. *Clin Cancer Res* 2001;7:3519-25.
15. Zajchowski DA, Bartholdi MF, Gong Y, et al. Identification of gene expression profiles that predict the aggressive behavior of breast cancer cells. *Cancer Res* 2001;61:5168-78.
16. Notterman DA, Alon U, Sierk AJ, Levine AJ. Transcriptional gene expression profiles of colorectal adenoma, adenocarcinoma, and normal tissue examined by oligonucleotide arrays. *Cancer Res* 2001;61:3124-30.
17. Zhao YL, Piao CQ, Hei TK. Tumor suppressor function of Betaig-h3 gene in radiation carcinogenesis. *Adv Space Res* 2003;31:1575-82.
18. Skonier J, Bennett K, Rothwell V, et al.  $\beta$ ig-h3: a transforming growth factor- $\beta$ -responsive gene encoding a secreted protein that inhibits cell attachment *in vitro* and suppresses the growth of CHO cells in nude mice. *DNA Cell Biol* 1994;13:571-84.
19. Schramm A, Schulte JH, Klein-Hitpass L, et al. Prediction of clinical outcome and biological characterization of neuroblastoma by expression profiling. *Oncogene* 2005;24:7902-12.
20. Schulte JH, Schramm A, Klein-Hitpass L, et al. Microarray analysis reveals differential gene expression patterns and regulation of single target genes contributing to the opposing phenotype of TrkA- and TrkB-expressing neuroblastomas. *Oncogene* 2005;24:165-77.
21. Tasanen K, Tunggal L, Chometon G, Bruckner-Tuderman L, Aumailley M. Keratinocytes from patients lacking collagen XVII display a migratory phenotype. *Am J Pathol* 2004;164:2027-38.
22. Korff T, Augustin HG. Integration of endothelial cells in multicellular spheroids prevents apoptosis and induces differentiation. *J Cell Biol* 1998;143:1341-52.
23. Hecht M, Papoutsi M, Tran HD, Wilting J, Schweigerer L. Hepatocyte growth factor/c-Met signaling promotes the progression of experimental human neuroblastomas. *Cancer Res* 2004;64:6109-18.
24. Schwab M, Alitalo K, Klempnauer KH, et al. Amplified DNA with limited homology to myc cellular oncogene is shared by human neuroblastoma cell lines and a neuroblastoma tumour. *Nature* 1983;305:245-8.
25. Ohno S, Noshiro M, Makihira S, et al. RGD-CAP ( $\beta$ ig-h3) enhances the spreading of chondrocytes and fibroblasts via integrin  $\alpha(1)\beta(1)$ . *Biochim Biophys Acta* 1999;1451:196-205.
26. Park SW, Bae JS, Kim KS, et al.  $\beta$ ig-h3 promotes renal proximal tubular epithelial cell adhesion, migration and proliferation through the interaction with  $\alpha_3\beta_1$  integrin. *Exp Mol Med* 2004;36:211-9.
27. Mangeat P, Roy C, Martin M. ERM proteins in cell adhesion and membrane dynamics. *Trends Cell Biol* 1999;9:187-92.
28. Bretscher A, Edwards K, Fehon RG. ERM proteins and merlin: integrators at the cell cortex. *Nat Rev Mol Cell Biol* 2002;3:586-99.
29. Ross EM, Wilkie TM. GTPase-activating proteins for heterotrimeric G proteins: regulators of G protein signaling (RGS) and RGS-like proteins. *Annu Rev Biochem* 2000;69:795-827.
30. Izumi H, Takahashi C, Oh J, Noda M. Tissue factor pathway inhibitor-2 suppresses the production of active matrix metalloproteinase-2 and is down-regulated in cells harboring activated ras oncogenes. *FEBS Lett* 2000;481:31-6.
31. Herman MP, Sukhova GK, Kiesel W, et al. Tissue factor pathway inhibitor-2 is a novel inhibitor of matrix metalloproteinases with implications for atherosclerosis. *J Clin Invest* 2001;107:1117-26.
32. Jin M, Udagawa K, Miyagi E, et al. Expression of serine proteinase inhibitor PP5/TFPI-2/MSPI decreases the invasive potential of human choriocarcinoma cells *in vitro* and *in vivo*. *Gynecol Oncol* 2001;83:325-33.
33. Yan C, Wang H, Boyd DD. ATF3 represses 72-kDa type IV collagenase (MMP-2) expression by antagonizing p53-dependent trans-activation of the collagenase promoter. *J Biol Chem* 2002;277:10804-12.
34. Logan CY, Nusse R. The Wnt signaling pathway in development and disease. *Annu Rev Cell Dev Biol* 2004;20:781-810.
35. Bañico A, Liu G, Goldin L, Harris V, Aaronson SA. An autocrine mechanism for constitutive Wnt pathway activation in human cancer cells. *Cancer Cell* 2004;6:497-506.
36. Oh JE, Kook JK, Min BM.  $\beta$ ig-h3 induces keratinocyte differentiation via modulation of involucrin and transglutaminase expression through the integrin  $\alpha_3\beta_1$  and the phosphatidylinositol 3-kinase/Akt signaling pathway. *J Biol Chem* 2005;280:21629-37.
37. Yamamura J, Miyoshi Y, Tamaki Y, et al. mRNA expression level of estrogen-inducible gene,  $\alpha$ 1-antichymotrypsin, is a predictor of early tumor recurrence in patients with invasive breast cancers. *Cancer Sci* 2004;95:887-92.
38. Gagliardi AD, Kuo EY, Raulic S, Wagner GF, DiMattia GE. Human stanniocalcin-2 exhibits potent growth-suppressive properties in transgenic mice independently of growth hormone and IGFs. *Am J Physiol Endocrinol Metab* 2005;288:E92-105.
39. Wong CK, Yeung HY, Mak NK, DiMattia GE, Chan DK, Wagner GF. Effects of dibutyryl cAMP on stanniocalcin and stanniocalcin-related protein mRNA expression in neuroblastoma cells. *J Endocrinol* 2002;173:199-209.
40. Jin C, Li H, Ugai H, Murata T, Yokoyama KK. Transcriptional regulation of the c-jun gene by AP-1 repressor protein JDP2 during the differentiation of F9 cells. *Nucleic Acids Res Suppl* 2002;2:97-8.
41. Heinrich R, Livne E, Ben-Izhak O, Aronheim A. The c-Jun dimerization protein 2 inhibits cell transformation and acts as a tumor suppressor gene. *J Biol Chem* 2004;279:5708-15.
42. Ostrovsky O, Bengal E, Aronheim A. Induction of terminal differentiation by the c-jun dimerization protein JDP2 in C2 myoblasts and rhabdomyosarcoma cells. *J Biol Chem* 2002;277:40043-54.
43. Bird CH, Blink EJ, Hirst CE, et al. Nucleocytoplasmic distribution of the ovalbumin serpin PI-9 requires a nonconventional nuclear import pathway and the export factor Crm1. *Mol Cell Biol* 2001;21:5396-407.
44. Bird CH, Sutton VR, Sun J, et al. Selective regulation of apoptosis: the cytotoxic lymphocyte serpin proteinase inhibitor 9 protects against granzyme B-mediated apoptosis without perturbing the Fas cell death pathway. *Mol Cell Biol* 1998;18:6387-98.
45. Kim JE, Kim SJ, Jeong HW, et al. RGD peptides released from  $\beta$ ig-h3, a TGF- $\beta$ -induced cell-adhesive molecule, mediate apoptosis. *Oncogene* 2003;22:2045-53.